Ab Initio Structure of *p*-Shell Hypernuclei

R. Wirth, R. Roth

published in

NIC Symposium 2018
K. Binder, M. Müller, A. Trautmann (Editors)

Forschungszentrum Jülich GmbH,
John von Neumann Institute for Computing (NIC),
Schriften des Forschungszentrums Jülich, NIC Series, Vol. 49,
ISBN 978-3-95806-285-6, pp. 205.
http://hdl.handle.net/2128/17544

Ab Initio Structure of p-Shell Hypernuclei

Roland Wirth and Robert Roth

Institut für Kernphysik, Technische Universität Darmstadt, 64289 Darmstadt, Germany
E-mail: {*roland.wirth,robert.roth*}*@physik.tu-darmstadt.de*

We develop an extension of the No-Core Shell Model (NCSM) to hypernuclei. We outline the formalism of the NCSM and the computational methods needed to solve the quantum many-body problem. A major computational challenge is the rapid growth of the model space with the number of particles in the system and the model-space truncation parameter. We mitigate this by introducing an importance-truncation scheme that restricts the model space to the parts that are deemed important for the problem at hand. Also, to speed up convergence with the model-space truncation, we perform a Similarity Renormalisation Group transformation on the Hamiltonian before the calculation. We close with example calculations of two p-shell hypernuclei and discuss the implications of our results on the construction of hyperon-nucleon interactions as well as on neutron-star physics.

1 Introduction

The theory of the strong interaction, Quantum Chromodynamics (QCD), which acts inside atomic nuclei, describes interactions between quarks and gluons. There are six quark types (flavours), of which only the lightest two, the up and down quarks, make up the proton and neutron, and thus all atomic nuclei. Using energetic particles, however, one can replace one of the up and down quarks inside a proton or neutron (nucleon) with a strange quark – the lightest of the other flavours – and create a hyperon. If the hyperon happens to be bound in an atomic nucleus, because the original nucleon was or because the hyperon was captured by a nucleus, the system becomes a hypernucleus.

The lightest hyperons are the Λ^0 and $\Sigma^{\pm,0}$. One obtains the $\Xi^{0,-}$ hyperons by substituting an additional strange quark. All these hyperons have spin $1/2$ and behave like fermions. Due to them containing strange quarks, they are distinguishable from the nucleons. The number of strange quarks defines the *strangeness* of a hyperon (traditionally defined with a minus sign), so that the Λ and Σ hyperons have strangeness $\mathcal{S} = -1$ while the Ξ have $\mathcal{S} = -2$.

The up and down quarks are much lighter than the strange quark so that hyperons decay quickly via weak processes. The typical lifetime of a strange hyperon is 10^{-10} s. Although this time scale is short compared to the lifetimes of most unstable nuclei, it is orders of magnitude longer than the time scales of strong and electromagnetic processes. Thus, hypernuclear energy levels are well defined and electromagnetic transitions between them can be measured.

The first experimental detection of a hypernucleus was by Danysz and Pniewski (1953)[1] in a balloon-flown emulsion stack, in which the hypernucleus was produced by a cosmic ray. Since then, a multitude of experiments have been conducted using kaon beams, which already carry strangeness, or pion and electron beams, where a strange-antistrange pair is created in the production reaction. The early experiments used emulsion stacks as target, where the tracks of the produced particles can be used to infer properties of the produced hypernuclei[2,3]. More recent spectrometer experiments can measure hypernuclear ground and excited states with high resolution via their decay[4] or reaction products[5–7]. Also, direct measurement of the gamma rays produced by the deexcitation of the hypernucleus after production provides excitation spectra with very high precision[8–11].

Hypernuclei challenge our understanding of the strong interaction in multiple ways: First, the interaction among hyperons and nucleons cannot currently be computed realistically from the interactions among the quarks themselves, which are described by QCD. This is rooted in the complex internal structure of these objects and in QCD exhibiting *confinement*, which prevents single quarks and gluons from being observed. Efforts employing lattice QCD to generate synthetic scattering data[12] or to compute the potential directly[13] are underway but currently limited by unphysical quark masses or insufficient statistics. Second, QCD interactions exhibit flavour symmetry, i.e., an invariance of observables under permuting, or building certain linear combinations of, the different quark flavours. However, this symmetry is broken by the different quark masses, creating a rich structure in hypernuclear spectra.

With chiral effective field theory (χEFT), we have a systematic symmetry-based connection between QCD and the hyperon-nucleon and nucleonic interactions in the form of a low-momentum expansion with parameters fitted to experimental data[14,15]. Together with recent developments in unitary transformations accelerate convergence with respect to the size of the model space, this sparked a tremendous development of *ab initio* many-body methods, i.e., methods that provide systematically improvable solutions to the quantum many-body problem, for nonstrange nuclei[16].

The hyperon-nucleon interaction is not well-known because scattering experiments, which are the experimental foundation on which all models of the nucleon-nucleon and hyperon-nucleon interactions are built, are intrinsically very challenging due to the very short hyperon lifetime. On the other hand, there is a wealth of data on hypernuclear observables from over 50 years of experiments. The χEFT-based potentials provide an accurate description of light nuclei, so the hyperon-nucleon interaction is the main source of uncertainty. *Ab initio* methods provide a systematic link between the ill-constrained interaction and the hypernuclear data. We can use this link to better constrain the hyperon-nucleon interaction and provide predictions for observables that have not been measured or are not experimentally accessible.

2 Importance-Truncated No-Core Shell Model

Based on this, we extended a versatile many-body method, the Importance-Truncated No-Core Shell Model (IT-NCSM)[17–19], to the treatment of $\mathcal{S} = -1$ hypernuclei. Contrary to *ab initio* methods aimed at few-body systems, the IT-NCSM describes the many-body system in terms of laboratory-frame instead of relative (Jacobi) coordinates. This is advantageous because we can trivially ensure antisymmetry of the wave function, a defining property of a system of fermions, by employing a basis of Slater determinants. The antisymmetrisation procedure for approaches working in Jacobi coordinates becomes increasingly demanding with particle number, effectively limiting the size of tractable problems to $A \leq 7$ particles[20]. The tradeoff for the simple antisymmetrisation is that the model space contains the centre-of-mass (c.m.) degrees of freedom, which are redundant because a (hyper-)nucleus is self-bound.

The IT-NCSM basis consists of Slater determinants of harmonic-oscillator (HO) single-particle states for the nucleons and hyperons. This infinite basis is made finite by introducing a truncation parameter N_{max} to which the number of HO excitation quanta relative to the lowest Pauli-allowed state is limited. This particular choice of basis and truncation decouples the intrinsic from the c.m. degrees of freedom, making the IT-NCSM exactly equivalent to an analogous formulation in terms of Jacobi coordinates. Since our problem is rotationally invariant and preserves parity, we only include states with a certain projection M of the total angular momentum and either positive or negative parity into the basis.

With the basis fixed, we compute a matrix representation of the hypernuclear Hamiltonian

$$\boldsymbol{H} = \Delta\boldsymbol{M} + \boldsymbol{T}_{\text{int}} + \boldsymbol{V}_{NN} + \boldsymbol{V}_{3N} + \boldsymbol{V}_{YN} + \boldsymbol{V}_{YNN}, \tag{1}$$

which consists of a term accounting for the mass differences between the proton and the neutron and among the hyperons, the intrinsic kinetic energy of the system, and nucleon-nucleon, three-nucleon, hyperon-nucleon and hyperon-nucleon-nucleon interactions. The many-body matrix elements are computed from the two- and three-body matrix elements of the interactions using Slater-Condon rules.

Here, another advantage of Slater determinant bases comes into play: an n-body interaction can only connect Slater determinants that differ by n single-particle states at most. This renders the matrix representation of the Hamiltonian very sparse; moreover, the sparsity pattern is easy to predict simply from the operator rank and the two Slater determinants. Basis choices that exploit more symmetries of the Hamiltonian, such as rotational invariance or isospin, often have much smaller basis dimensions but produce denser matrices.

We are interested in the low-lying eigenvalues and corresponding eigenvectors of the Hamilton matrix. To get them, we use the implicitly-restarted Arnoldi method as implemented in the ARPACK library[21]. The eigenvalues are approximations to the absolute binding energies of the states, the differences to the lowest eigenvalue are excitation energies. Other observables can be calculated by taking matrix elements of the operator corresponding to the observable between the computed eigenstates.

The eigenvalues and eigenvectors are approximations to the eigenenergies and eigenstates of the Hamiltonian because the model space is truncated. Ritz' variational principle, however, ensures that the eigenvalues are upper bounds to the exact eigenenergies, and the eigenvalues converge to the exact eigenenergies with increasing N_{max}. Thus, we do not just pick a single model-space truncation N_{max} but solve the eigenvalue problem for a sequence of N_{max} values until convergence is achieved or sufficient to warrant an extrapolation to the infinite model space.

The limiting factor of the No-Core Shell Model is the size of the basis, which increases rapidly with N_{max} and the number of particles A. In hypernuclei, the problem is exacerbated by a property of the hyperon-nucleon interaction: by interacting with a nucleon, a Λ hyperon can be converted into a Σ hyperon and vice versa. This necessitates the inclusion of Λ and Σ single-particle states into the model space, further increasing its size. Even for a light hypernucleus such as ${}^{7}_{\Lambda}\text{Li}$ the model-space dimension at $N_{\text{max}} = 12$ exceeds 10^9 basis states, which is at the limit of model spaces tractable with current computers when the Hamiltonian includes three-body forces.

Since we are only interested in a few (≤ 10) of the lowest eigenpairs, a lot of the basis states will have a very small overlap with these states of interest (target states). These irrelevant basis states can be removed from the model space without affecting the target eigenpairs much. This is the core idea of importance truncation. To find the irrelevant states without solving the eigenvalue problem itself, we employ Multi-Configurational Perturbation Theory (MCPT). The first-order MCPT correction to a reference state $|\Psi_{\text{ref}}\rangle \in \mathcal{M}_{\text{ref}}$ in terms of the basis states $|\Phi_i\rangle$ is

$$|\Psi^{(1)}\rangle = -\sum_{i \notin \mathcal{M}_{\text{ref}}} \frac{\langle \Phi_i | \boldsymbol{H} | \Psi_{\text{ref}} \rangle}{\Delta\epsilon_i} |\Phi_i\rangle \equiv \sum_{i \notin \mathcal{M}_{\text{ref}}} \kappa_i |\Phi_i\rangle, \tag{2}$$

where $\Delta\epsilon_i$ is the HO excitation energy of the basis state $|\Phi_i\rangle$. The reference state is from a diagonalisation in a smaller model space $\mathcal{M}_{\text{ref}}$ and the κ_i are a first-order perturbative estimate of the importance of the corresponding basis state.

To build the importance-truncated model space we only include states with $|\kappa_i| \geq \kappa_{\text{min}}$. If we do so in a sequential scheme, where the model space for the next $N_{\text{max}} = N + 2$ step is built using the results of the diagonalisation in $N_{\text{max}} = N$, the construction of the new basis states is especially simple because we need only consider substitutions of up to two single-particle states (2p-2h excitations) on each of the current basis states. This breeding process – creating candidate Slater determinants and estimating their importance – is computationally expensive and consumes up to a third of the total computing time, but it reduces the basis dimension by several orders of magnitude: in the case of ${}^{7}_{\Lambda}$Li at $N_{\text{max}} = 12$ the reduction is from $1.6 \cdot 10^9$ to $1.2 \cdot 10^7$ for the smallest threshold, i.e., the largest space used.

The effect of the neglected basis states on observables is small but not negligible. To account for it, we select a range of κ_{min} thresholds for which we solve the eigenvalue problem and compute observables, and extrapolate $\kappa_{\text{min}} \to 0$ using a low-order polynomial. The sequence of diagonalisations is done efficiently by starting from the lowest threshold and moving up, removing the rows and columns from the Hamilton matrix that belong to basis states falling below the current threshold.

3 Similarity Renormalisation Group

Even with the extended reach of the IT-NCSM it is impossible to achieve satisfactory convergence when using the interactions as is. This is caused by parts of the interaction that couple low- and high-energy states and thus can only be accommodated in very large model spaces. Unitary transformations are a means to lower the size of the model spaces required for convergence while keeping all observables invariant.

A versatile class of transformations is provided by the Similarity Renormalisation Group (SRG)[22–24]. A general unitarily transformed Hamiltonian is written as

$$\boldsymbol{H}(\alpha) = \boldsymbol{U}^{\dagger}(\alpha) \boldsymbol{H} \boldsymbol{U}(\alpha), \tag{3}$$

where α is a continuous parameter controlling the transformation, and differentiating with respect to this flow parameter yields the SRG flow equation

$$\frac{\mathrm{d}\boldsymbol{H}(\alpha)}{\mathrm{d}\alpha} = [\boldsymbol{\eta}(\alpha), \boldsymbol{H}(\alpha)], \tag{4}$$

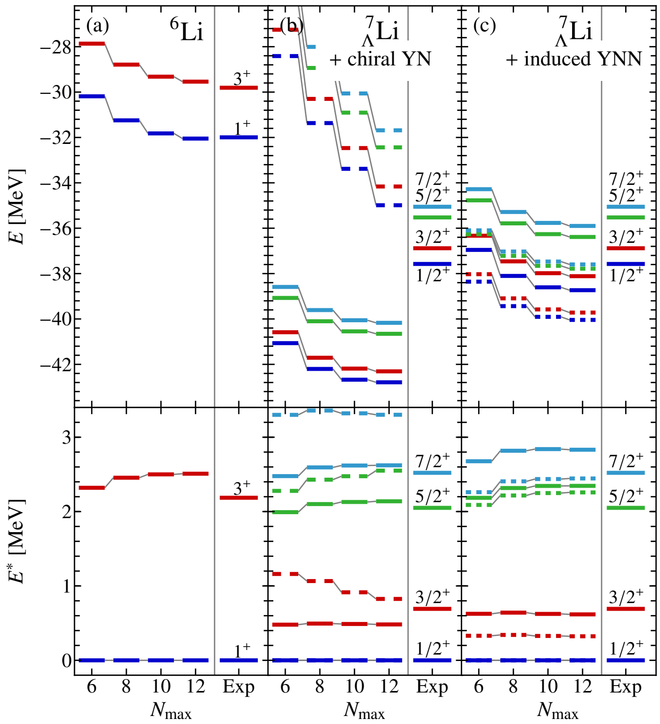

Figure 1. Absolute and excitation energies of (a) ^{6}Li and (b-c) its daughter hypernucleus $^7_\Lambda$Li. The middle panel shows calculations without YNN terms for the unevolved (dashed lines) and evolved (solid lines) YN interaction (700 MeV/c cutoff). The right panel gives results with induced YNN terms for the 600 MeV/c (dotted lines) and 700 MeV/c cutoffs (solid lines).

where $[X, Y] = XY - YX$ denotes a commutator. The anti-Hermitian generator $\boldsymbol{\eta}(\alpha) = -\boldsymbol{U}^\dagger(\alpha)(\mathrm{d}\boldsymbol{U}(\alpha)/\mathrm{d}\alpha)$ can be tailored to achieve the desired behaviour. In our case we use $\boldsymbol{\eta}(\alpha) = (2m_N)^2[\boldsymbol{T}_{\text{int}}, \boldsymbol{H}(\alpha)]$, with the nucleon mass m_N to fix the unit of α, to drive the Hamiltonian to a band-diagonal form in HO basis, decoupling the high- from the low-energy states.

The improved convergence comes at a price: even if $\boldsymbol{H}$ consists only of two-body interactions, $\boldsymbol{H}(\alpha)$ will have up to A-body terms. To exactly preserve unitarity of the transformation, we would have to take all these induced many-body terms into account, which is computationally infeasible. Fortunately, truncating the induced interactions beyond three-body terms suffices so that the dependence of observables on the flow parameter α are small[25].

The three-body terms are captured by performing the SRG transformation in three-body space. Analogous to the IT-NCSM we choose a HO basis in which we represent the Hamiltonian and the other relevant operators, but we use symmetry-adapted basis states and Jacobi coordinates in order to have model spaces large enough to converge the SRG evolution. In basis representation the flow equation becomes a set of matrix ODE initial-value problems – because the representation of the Hamiltonian is a block-diagonal ma-

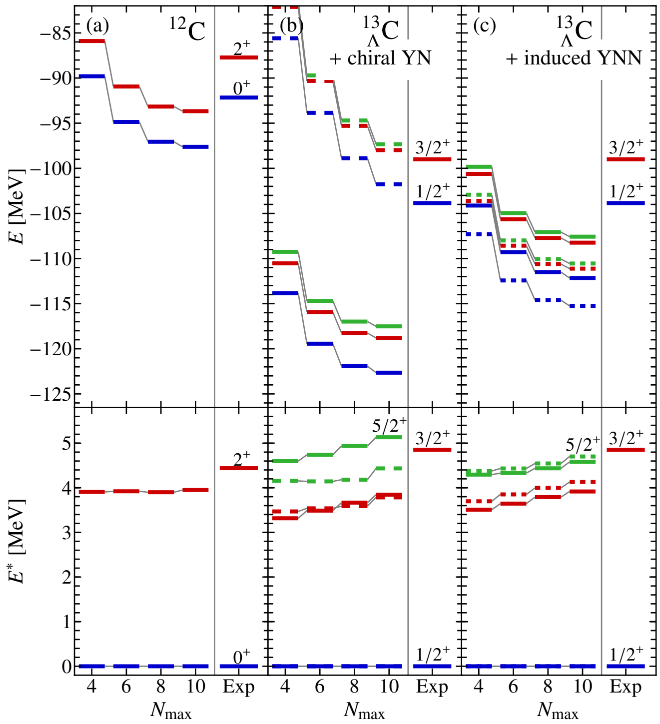

Figure 2. Same as Fig. 1, but for ^{12}C and $^{13}_{\Lambda}$C.

trix – with the largest block having approximately $(5 \cdot 10^4)^2$ unknowns. To solve this efficiently, we distribute the matrix among several compute nodes and make extensive use of level-3 BLAS routines, overlapping computation of the matrix products with transfer of matrix parts among the nodes where possible.

4 Results

For the following computations we use a standard nucleonic Hamiltonian, consisting of a next-to-next-to-next-to-leading-order (N^{3}LO) two-nucleon interaction by Entem and Machleidt[26], an N^{2}LO three-nucleon interaction by Navrátil[27], and a LO hyperon-nucleon interaction by Polinder *et al.*[28] The nucleonic part provides a good description of light nuclei. Unless stated otherwise, the Hamiltonian is SRG-evolved to a flow parameter of $\alpha = 0.08\,\text{fm}^4$ and the frequency of the HO basis is $\hbar\Omega = 20\,\text{MeV}$.

The calculations we present here are the first of their kind for p-shell nuclei that employ a chiral Hamiltonian with induced three-body interactions taken into account. They were first published in Ref. 29 and are based on our work from Ref. 30.

Fig. 1 shows the absolute and excitation energies of ^{6}Li and its daughter hypernucleus $^7_{\Lambda}$Li. While the absolute energies of ^{6}Li are not quite converged, the excitation energy of the 3^+ state is and comes out about 300 keV too high. Moving on to the results for the hypernucleus ${}^{7}_{\Lambda}$Li computed without (induced) YNN terms we see that the unevolved interaction is very far from convergence, both for the spectra and absolute energies. An SRG evolution is essential to accelerate convergence and be able to reliably extrapolate the energies. The SRG-evolved interaction drastically improves convergence but creates a significant overbinding and lowers the splitting of the ground-state doublet compared to experiment. The addition of the induced YNN terms (right panel) shifts the results closer to experiment by reducing the overbinding and increasing the splitting in the ground-state doublet. The excited-state doublet is now $300\,\mathrm{keV}$ above the experimental values, but this deficiency is rooted in the description of the nucleonic part. Overall, we achieve remarkable agreement with experiment for this hypernucleus. However, the results still depend on a parameter of the YN interaction: the regulator cutoff. Dependence on the cutoff should decrease with increasing χEFT order and, as expected, is strong for the leading-order interaction employed here. This can be seen by comparing the results for the $600\,\mathrm{MeV}/c$ and $700\,\mathrm{MeV}/c$ cutoffs. The lower cutoff produces additional overbinding and small doublet splittings.

The situation for ^{12}C and ${}^{13}_{\Lambda}$C, shown in Fig. 2, is similar, except that some overbinding is already present in the nucleonic calculation. Remarkably, the spectra depend less strongly on the cutoff than in ${}^{7}_{\Lambda}$Li. Evidence from experiment[11] suggests that the $3/2^+$ state is actually the upper level of the excited-state doublet instead of the lower one as it is predicted by our calculation. Information about such systematic deviations can be used to guide the development of improved interaction models and is only really accessible in *ab initio* calculations. These calculations do not make any assumption about the structure of the calculated states; thus, all discrepancies have to originate from the interaction and cannot be traced back to modelling errors in the many-body method.

The physics of hypernuclei also plays a role in the description of neutron stars where strangeness production can occur at high densities. Better understanding and constraining the YN interaction and understanding the origin of scheme- and scale-dependent many-body terms, such as the SRG-induced YNN terms, will help build better models of these objects.

Acknowledgements

The authors gratefully acknowledge the computing time granted by the John von Neumann Institute for Computing (NIC) and provided on the supercomputer JURECA at Jülich Supercomputing Centre (JSC).

References

1. M. Danysz and J. Pniewski, Phil. Mag. **44**, 348–350, 1953.
2. H. Takahashi, J. K. Ahn, H. Akikawa, et al., Phys. Rev. Lett. **87**, 212502, 2001.
3. D. H. Davis, Nucl. Phys. A **754**, 3–13, 2005.
4. A. Esser, S. Nagao, F. Schulz, et al., Phys. Rev. Lett. **114**, 232501, 2015.
5. P. K. Saha, T. Fukuda, W. Imoto, et al., Phys. Rev. Lett. **94**, 052502, 2005.
6. F. Cusanno, G. Urciuoli, A. Acha, et al., Phys. Rev. Lett. **103**, 202501, 2009.
7. S. N. Nakamura, A. Matsumura, Y. Okayasu, et al., Phys. Rev. Lett. **110**, 012502, 2013.

8. H. Tamura, K. Tanida, D. Abe, et al., Phys. Rev. Lett. **84**, 5963–6, 2000.
9. K. Tanida, H. Tamura, D. Abe, et al., Phys. Rev. Lett. **86**, 1982–1985, 2001.
10. H. Akikawa, S. Ajimura, R. Chrien, et al., Phys. Rev. Lett. **88**, 082501, 2002.
11. O. Hashimoto and H. Tamura, Prog. Part. Nucl. Phys. **57**, 564–653, 2006.
12. S. R. Beane, P. F. Bedaque, T. C. Luu, et al., Nucl. Phys. A **794**, 62–72, 2007.
13. H. Nemura, S. Aoki, T. Doi, et al., *Lambda-Nucleon and Sigma-Nucleon interactions from lattice QCD with physical masses*, in: 34th Annu. Int. Symp. Lattice F. Theory, PoS(LATTICE2016) 101, 2017.
14. E. Epelbaum, H.-W. Hammer, and U.-G. Meißner, Rev. Mod. Phys. **81**, 1773–1825, 2009.
15. R. Machleidt and D. Entem, Phys. Rep. **503**, 1–75, 2011.
16. M. Hjorth-Jensen, M. P. Lombardo, and U. van Kolck, (Eds.), *An Advanced Course in Computational Nuclear Physics*, vol. 936 of *Lecture Notes in Physics*, Springer International Publishing, 2017.
17. R. Roth, Phys. Rev. C **79**, 064324, 2009.
18. R. Roth, J. Langhammer, A. Calci, et al., Phys. Rev. Lett. **107**, 072501, 2011.
19. B. R. Barrett, P. Navrátil, and J. P. Vary, Prog. Part. Nucl. Phys. **69**, 131–181, 2013.
20. S. Liebig, U.-G. Meißner, and A. Nogga, Eur. Phys. J. A **52**, 103, 2016.
21. R. B. Lehoucq, D. C. Sorensen, and C. Yang, "ARPACK Library", 1997.
22. F. J. Wegner, Nucl. Phys. B (Proc. Suppl.) **90**, 141–146, 2000.
23. R. Roth, S. Reinhardt, and H. Hergert, Phys. Rev. C **77**, 064003, 2008.
24. S. Bogner, R. Furnstahl, and A. Schwenk, Prog. Part. Nucl. Phys. **65**, 94–147, 2010.
25. R. Roth, A. Calci, J. Langhammer, and S. Binder, Phys. Rev. C **90**, 024325, 2014.
26. D. R. Entem and R. Machleidt, Phys. Rev. C **68**, 041001, 2003.
27. P. Navrátil, Few-Body Syst. **41**, 117–140, 2007.
28. H. Polinder, J. Haidenbauer, and U.-G. Meißner, Nucl. Phys. A **779**, 244–266, 2006.
29. R. Wirth and R. Roth, Phys. Rev. Lett. **117**, 182501, 2016.
30. R. Wirth, D. Gazda, P. Navrátil, et al., Phys. Rev. Lett. **113**, 192502, 2014.